Journal of Molecular Histology (2027) 58:4
https://doi.org/10.1007/s10735-026-11061-1

ORIGINAL PAPER

Effects of vitrification techniques and intracellular cryoprotectant concentrations on dermal tissue cryopreservation in the Antillean manatee (*Trichechus manatus manatus*, Linnaeus, 1758)

Luanna Lorenna Vieira Rodrigues[1] · Leonardo Vitorino Costa de Aquino[1] · Pedro Rafael Ribeiro Assunção[1] · Yara Letícia Frutuoso e Silva[1] · Vinicius Dantas da Silva[1] · Maria Valéria de Oliveira Santos[1] · Radan Elvis Matias de Oliveira[2] · Moacir Franco de Oliveira[2] · Fábia de Oliveira Luna[3] · Fernanda Loffler Niemeyer Attademo[1,3] · Alexsandra Fernandes Pereira[1]

Received: 17 July 2026 / Accepted: 9 November 2026
© The Author(s) 2026

Abstract

Dermal tissue cryopreservation plays a key role in biodiversity conservation by enabling somatic resource banks for genetic preservation, functional studies, and biotechnological applications. While slow freezing is an established technique, vitrification offers a practical, field-adaptable alternative, particularly relevant for the Antillean manatee. Therefore, optimizing vitrification protocols and cryoprotectant combinations is essential for establishing dermal tissue banks. This study evaluated two vitrification techniques (direct cover vitrification, DCV, and direct vitrification in cryovials, DVC) using two intracellular cryoprotectant concentrations (3.0 M or 6.0 M ethylene glycol and dimethyl sulfoxide) for Antillean manatee dermis cryopreservation. Non-cryopreserved tissues and slow-frozen samples served as controls. All groups were assessed by histological and ultrastructural analyses and their ability to support fibroblast recovery. Histological evaluations showed that fibroblast density was preserved in DCV at both concentrations, with results comparable to fresh tissue and slow freezing. The collagen matrix was preserved only in DCV-6 M, whereas all vitrification protocols maintained normal elastic fiber organization. Despite preserving tissue architecture, fibroblast recovery was successful only in non-cryopreserved and slow-frozen samples, while vitrified tissues failed to support cell proliferation. Although DCV, particularly at 6 M, effectively preserves dermal structure, the tested vitrification protocols were insufficient to ensure fibroblast recovery.

Keywords Wildlife conservation biotechnology · Sirenians · Cryobank · Cryopreservation · Histological preservation · Cell recovery capacity

Introduction

The Antillean manatee (*Trichechus manatus manatus*, Linnaeus, 1758), recently classified as endangered, faces increasing threats from habitat degradation, anthropogenic pressures, and low intrinsic reproductive rates (Morales-Vela et al. 2024; Val et al. 2024). In this context, the development of complementary *ex situ in vitro* conservation strategies has become essential to support long-term species survival (Rodrigues et al. 2025a). Among these strategies, the establishment of somatic resource banks based on dermal tissues represents a valuable approach for preserving genetic material, enabling cellular studies, and supporting

✉ Alexsandra Fernandes Pereira
alexsandra.pereira@ufersa.edu.br

[1] Laboratory of Animal Biotechnology, Department of Biosciences, Federal Rural University of Semi-Arid, Av. Francisco Mota, 572, Costa e Silva, Mossoró, RN 59625-900, Brazil

[2] Laboratory of Applied Animal Morphophysiology, Department of Animal Science, Federal Rural University of Semi-Arid, Mossoró, RN, Brazil

[3] National Center for Research and Conservation of Aquatic Mammals by Chico Mendes Institute for Biodiversity Conservation, Santos, SP, Brazil

Published online: 18 November 2026

future reproductive and biotechnological applications (Boroda et al. 2020; Rodrigues et al. 2025b).

Cryopreservation of dermal tissue enables long-term storage of viable somatic cells, particularly fibroblasts, which can be used in functional assays, genome conservation, and advanced assisted reproductive techniques (Brereton et al. 2025; Olindo et al. 2024). Slow freezing is currently the most widely applied method for somatic tissue cryopreservation and has shown consistent success across several mammalian species (Engdawork et al. 2024; Fernandes et al. 2023; Olindo et al. 2024). However, its reliance on controlled-rate freezing equipment limits its applicability under field conditions, which are often required for wildlife species, such as the Antillean manatee (Rodrigues et al. 2025a). Vitrification has emerged as a promising alternative due to its simplicity, rapid execution, and reduced infrastructure requirements (Brereton et al. 2025; Costa et al. 2020; Viana et al. 2023).

In previous studies (Nascimento et al. 2023a, b), we evaluated solid-surface vitrification (SSV) using different cryoprotectant concentrations (3.0 M ethylene glycol (EG) plus 3.0 M dimethyl sulfoxide (Me_2SO); 1.5 M EG plus 1.5 M Me_2SO; 3.0 M EG; or 3.0 M Me_2SO) and compared its efficiency with slow freezing for the cryopreservation of Antillean manatee dermal tissue. These studies demonstrated that, despite partial preservation of tissue architecture, SSV-vitrification protocols tested were unable to support fibroblast recovery after culture, whereas slow freezing consistently maintained cell viability and proliferative capacity.

Given the inefficiency of SSV for this species, it is necessary to investigate alternative vitrification techniques that preserve tissue structural integrity and enable subsequent cell recovery, even when different cryoprotectant solution compositions are used. Moreover, beyond the vitrification techniques themselves, cryopreservation depends on cryoprotectants to mitigate freezing-induced damage, including ice crystal formation, protein denaturation, and oxidative stress (Gao et al. 2026). Therefore, these techniques must be evaluated in combination with different cryoprotectant solutions to allow a more comprehensive and detailed assessment of cryopreservation protocols.

Numerous cryopreservation protocols and cryodevices have been developed and extensively investigated to enhance the viability and functionality of biological samples after storage (Amini and Benson 2023). Among these, direct cover vitrification (DCV) has been shown to preserve tissue architecture and allow fibroblast recovery after warming in porcine somatic samples (Zhang et al. 2023). This technique involves exposing samples to an equilibrium solution, then directly to liquid nitrogen before storage. In contrast, direct vitrification in cryovials (DVC) has been successfully applied with variable efficiencies to several mammalian species using somatic tissues (Borges et al. 2017; Costa et al. 2020). This approach does not include an equilibrium solution step, and the samples do not come into direct contact with liquid nitrogen. Although the protocol differences between DCV and DVC are subtle, distinct biological samples exhibit varying sensitivities to cooling rates, and both excessively rapid and excessively slow cooling can induce irreversible damage (Pan and Zhang 2026). Consequently, even minor variations in vitrification protocols may be sufficient to determine whether a technique is successful or not for a given sample. In this context, a comprehensive evaluation and determination of optimal cooling rates for different biological materials are essential to improve cryopreservation outcomes.

Therefore, the study aimed to expand upon previous findings by evaluating alternative vitrification techniques and intracellular cryoprotectant concentrations to improve dermal tissue preservation in the Antillean manatee. Specifically, we compared DCV and DVC using two cryoprotectant concentrations (1.5 M EG plus 1.5 M Me_2SO and 3.0 M EG plus 3.0 M Me_2SO) with slow freezing and non-cryopreserved tissues as controls. Tissue integrity, ultrastructure, and fibroblast recovery were assessed to determine whether modifications to vitrification methodology could overcome previous limitations and optimize somatic tissue banking for this endangered species.

Materials and methods

Ethical considerations

This study was approved by the Animal Use Ethics Committee of the Federal Rural Semi-Arid (CEUA/UFERSA, protocol no. 23091.010755/2019-32) and authorized by the Chico Mendes (ICMBio, license no. 71804-1).

Media and chemicals

Dulbecco's modified minimal essential medium: F-12 nutrient mixture (DMEM/F-12), fetal bovine serum (FBS), and antibiotic-antimycotic solution were obtained from Gibco-BRL (Carlsbad, CA, USA). All other chemicals were purchased from Sigma-Aldrich Chemical Co. (St. Louis, MO, USA).

Animals and dermis collection

Five individuals (males and females) were included in this study. Four individuals were stranded animals—three calves and one juvenile—that were rescued and transferred to the Advanced Base of the National Center for Research and Conservation of Aquatic Mammals, operated by the Chico

Mendes Institute for Biodiversity Conservation (ICMBio/CMA; 7°48′33″ S, 34°50′19″ W), where they received veterinary care and underwent rehabilitation. The fifth individual was an adult born and raised in the same facility.

Abdominal skin samples were collected during routine animal handling procedures. The animals were manually restrained by trained handlers to ensure complete immobilization, as previously described (Nascimento et al. 2023a). Briefly, sample collection was performed following a rigorous aseptic protocol to minimize the risk of contamination. Initially, the sampling site underwent antisepsis through a triple cleansing procedure using sterile gauze pads and continuous, firm friction of the skin. A 10% povidone-iodine scrub and 70% ethanol were applied alternately. After the third application of 70% ethanol, a 2% alcoholic chlorhexidine solution (Riohex®, 2% chlorhexidine digluconate) was applied and maintained in contact with the skin for 3 min. Subsequently, 70% ethanol was reapplied to remove excess antiseptic, followed by drying of the area with sterile gauze. All personnel involved in the procedure wore disposable gloves and masks throughout sample collection. Dermal biopsies were obtained using an 8-mm sterile biopsy punch (Paramount Surgimed Ltd., New Delhi, India). Immediately after collection, the biopsies were briefly immersed in 70% ethanol and subsequently rinsed in culture medium consisting of DMEM/F-12 supplemented with 20% FBS and 2% antibiotic–antimycotic solution. The samples were transferred to sterile Falcon™ tubes containing the same culture medium and stored in a thermal container maintained at 4 °C during the sampling period. After the sample collection, all tissues were transported to the laboratory under controlled refrigeration (4 °C) and processed within 8 h of collection.

Dermis processing and experimental design

In the laboratory, the dermal biopsies were processed by carefully removing the epidermis mechanically using a sterile scalpel. The dermis was then sectioned into fragments of approximately 9.0 mm^3 (3 × 3 × 1 mm) using a sterile scalpel blade, as previously described (Nascimento et al. 2023b). A total of 54 fragments per animal were randomly allocated to non-cryopreserved and cryopreserved groups. Dermal fragments were cryopreserved using three protocols: slow freezing (SF), direct cover vitrification (DCV), and direct vitrification in cryovials (DVC). After warming, dermal tissues were assessed by histological analysis, ultrastructure, and their ability to support fibroblast recovery during culture. Non-cryopreserved samples were used as the control group.

Tissue cryopreservation

Dermis was cryopreserved for slow freezing (SF), direct cover vitrification (DCV), and direct vitrification in cryovials (DVC). All cryoprotectant solutions were prepared in a base medium consisting of Dulbecco's Modified Eagle Medium (DMEM) supplemented with 10% FBS and 0.25 M sucrose. For SF, the final cryopreservation solution contained 1.5 M Me_2SO and 1.5 M EG, corresponding to a total cryoprotectant concentration of 3.0 M, together with 0.25 M sucrose. The concentrations refer to the final concentrations of each component in the cryopreservation solution. For DCV, two different vitrification solutions were used: DCV-3 M (1.5 M Me_2SO with 1.5 M EG) and DCV-6 M (3 M Me_2SO with 3 M EG). For DVC, two different vitrification solutions were used: DVC-3 M (1.5 M Me_2SO with 1.5 M EG) and DVC-6 M (3 M Me_2SO with 3 M EG).

For SF, dermal fragments were placed in cryovials containing 2.0 mL of freezing solution and, within 30 min, transferred to a −80 °C freezer using a Mr. Frosty® freezing container (Thermo Scientific Nalgene, Rochester, USA), providing a controlled cooling rate of approximately −1 °C/min for 12 h. Subsequently, the cryovials were transferred to liquid nitrogen (−196 °C) for long-term storage, as previously described (Nascimento et al. 2023b).

The DCV was performed according to Zhang et al. (2023), with minor modifications. The dermal fragments were initially equilibrated for 5 min at 25 °C in an equilibrium solution composed of half the concentration of the vitrification solution used in each experimental group. Then, samples were transferred to the vitrification solution for an additional 5 min at the same temperature. Excess cryoprotectant solution was carefully removed with sterile gauze, and the fragments were immediately transferred to empty cryotubes. Liquid nitrogen was then added to the cryotubes, and after partial evaporation, the cryotubes were sealed and stored at −196 °C for long-term preservation.

For DVC, dermal fragments were placed directly into cryovials containing 2.0 mL of vitrification solution and incubated for 15 s at 25 °C. Immediately thereafter, the cryovials were plunged into liquid nitrogen (−196 °C) and stored at cryogenic temperatures, as described by Costa et al. (2020).

After six months of storage, the samples from all experimental groups were thawed. For this, the cryovials were removed from liquid nitrogen, kept at 25 °C for 1 min, and then subjected to a water bath at 37 °C for 3 min. Cryoprotectant removal was performed by washing the dermal fragments at room temperature in three solutions of DMEM supplemented with 10% FBS and sucrose in decreasing concentrations (0.50 M, 0.25 M, and 0.0 M) for 5 min each, as described by Nascimento et al. (2023b). After heating and

cryoprotectant removal, the fragments were immediately processed for subsequent analyses.

Histological processing and analyses

Dermal fragments were fixed in 4% paraformaldehyde prepared in phosphate-buffered saline (PBS). After fixation, samples were dehydrated through a graded ethanol series (70%, 80%, 95%, and 100%), cleared in xylene, embedded in paraffin, and sectioned at 5.0 µm thickness using a rotary microtome (Leica RM2125 RT, Leica Microsystems, Wetzlar, Germany), as previously described (Nascimento et al. 2023b).

Histological sections were stained with hematoxylin and eosin (H&E) (Nascimento et al. 2023b), Masson's trichrome (MT) (Su et al. 2023), and Weigert's trichrome (WT) (Anikienko et al. 2025), to evaluate fibroblast density, collagen matrix proportion (%), and elastic fiber content (%), respectively. For H&E analysis, 20 photomicrographs of randomly selected fields per slide were captured at 40× magnification. For MT and WT staining, 10 photomicrographs of random fields per slide were obtained at the same magnification.

All samples were examined using a light microscope (Leica DM500, Leica Microsystems, Wetzlar, Germany) equipped with a digital camera (Leica ICC50 HD, Leica Microsystems, Wetzlar, Germany). Quantitative analyses were performed using ImageJ (National Institutes of Health, Bethesda, MD, USA), according to previously established protocols (Nascimento et al. 2023b).

Processing and ultrastructural analyses

Scanning electron microscopy (SEM) was performed according to the method described by Aquino et al. (2024), with minor modifications. Dermal samples were fixed in 4% glutaraldehyde prepared in PBS. After fixation, the samples were rinsed three times for 10 min each in distilled water and subsequently post-fixed in 1% osmium tetroxide for 1 h and 15 min. Following post-fixation, samples were dehydrated through a graded ethanol series (7.5%, 15%, 30%, 50%, 70%, and 90%), with 5 min immersion at each concentration. The samples were washed three times for 10 min each in 100% ethanol. After dehydration, specimens were dried and sputter-coated with gold for surface metallization. Samples were examined using a scanning electron microscope (TESCAN VEGA3; Tescan Analytics, Fuveau, Bouches-du-Rhône, France), and representative images were acquired for ultrastructural analysis.

In vitro culture and fibroblast recovery

Dermal fragments destined for primary culture were sequentially washed in the following solutions: (I) DMEM/F12 supplemented with 20% FBS and 10% antibiotic–antimycotic solution; (II) DMEM/F12 supplemented with 20% FBS and 2% antibiotic–antimycotic solution; (III) 70% ethanol; and (IV) DMEM/F12 supplemented with 20% FBS and 2% antibiotic–antimycotic solution. After washing, eight fragments per animal (four fragments per culture dish) were plated in DMEM/F12 medium supplemented with 20% FBS and 2% antibiotic–antimycotic solution and incubated at 38.5 °C in a humidified atmosphere containing 6.5% CO_2 (Nascimento et al. 2023b).

Primary cultures were monitored daily using an inverted microscope (Leipzig IMx 400, Phoenix Optics, Germany), with complete medium replacement every 24 h. Cultured tissues were evaluated for time to attachment, detachment, and sub-confluence, as well as attachment and detachment rates (%), total culture duration, and the absence of microbial contamination, according to previously established criteria (Nascimento et al. 2023b).

Statistical analysis

Data on the animals were expressed as mean ± standard error (one animal/ replicate) and analyzed using the GraphPad software (GraphPad Software Inc., La Jolla, CA, USA). Significance was set at $p < 0.05$, and different superscript letters in the figures indicate statistically significant differences among groups. All results were verified for normality using the Shapiro–Wilk test and for homoscedasticity using Levene's test. Data on collagen and elastic matrix were analyzed by ANOVA (multiple comparisons) followed by the Tukey test. The results of fibroblast numbers were analyzed by Kruskal-Wallis and Dunn (multiple comparisons) tests.

Results

Effects of vitrification techniques on histological aspects

Histological analysis based on H&E staining (Fig. 1a–g) demonstrated that fibroblast density was preserved in the DCV-3 M (92 ± 24.5) and DCV-6 M (91 ± 17.8) groups, with values statistically comparable to those observed in the non-cryopreserved tissues (107 ± 22.9) and in tissues cryopreserved by SF (132 ± 26.1; Fig. 1b) ($p > 0.05$). These results indicate that, under the evaluated conditions, DCV vitrification effectively maintained dermal tissue architecture and fibroblast integrity following warming. In contrast, dermal

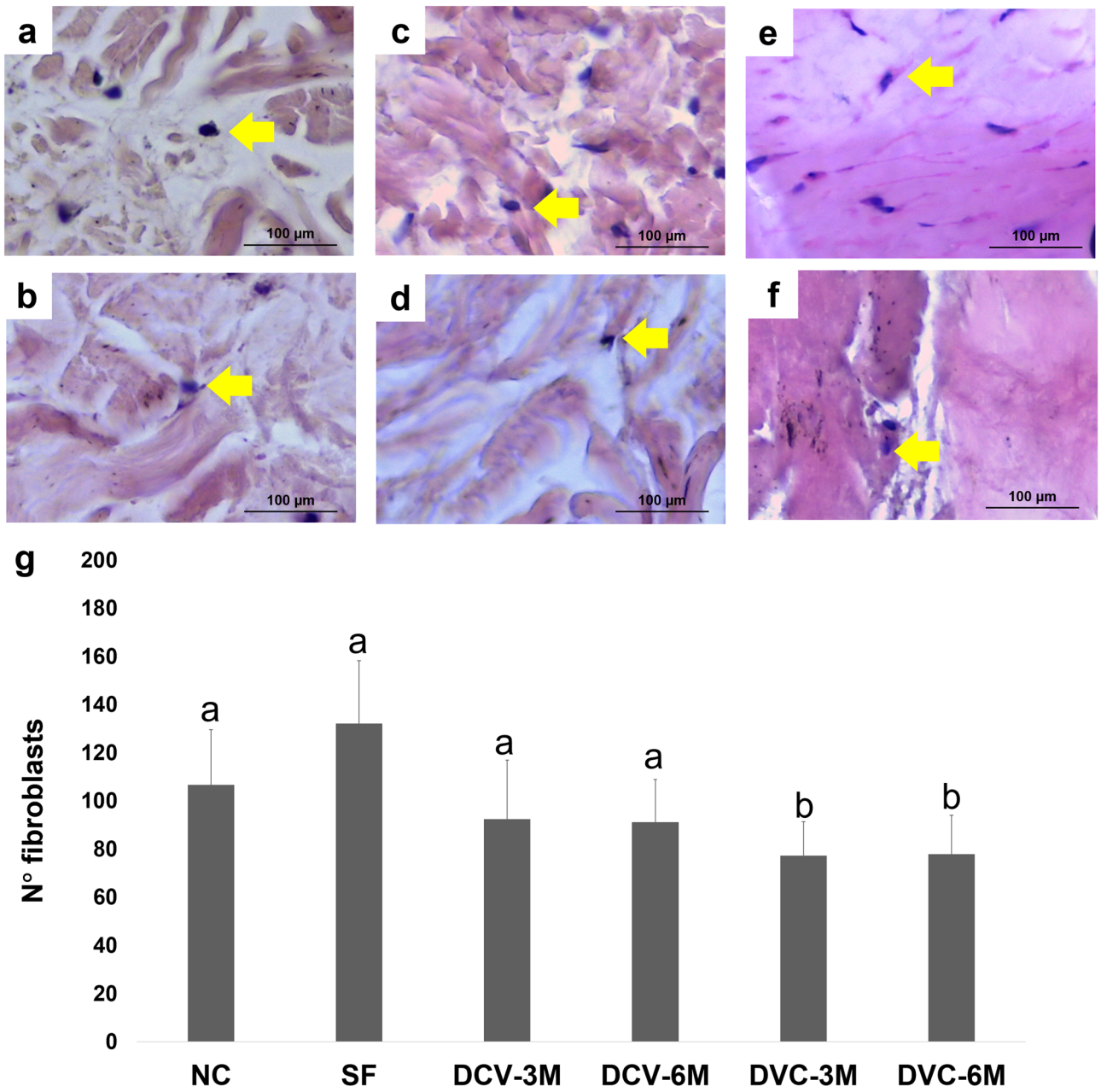


Fig. 1 Representative hematoxylin and eosin (H&E)-stained sections of the dermis of Antillean manatees showing fibroblast distribution following different tissue preservation methods: **a** non-cryopreserved (NC), **b** slow freezing (SF), **c** direct cover vitrification using 3 M cryoprotectant (DCV-3 M), **d** direct cover vitrification using 6 M cryoprotectant (DCV-6 M), **e** direct vitrification in cryovials using 3 M cryoprotectant (DVC-3 M), and **f** direct vitrification in cryovials using 6 M cryoprotectant (DVC-6 M). **g** Quantification of fibroblast abundance in the dermis of NC and cryopreserved groups. Yellow arrows indicate fibroblasts. Different superscript letters indicate statistically significant differences among groups ($p<0.05$). Scale bar = 100 µm, Magnification 40×

samples preserved by DVC exhibited a significant reduction in fibroblast density in both DVC-3 M (77 ± 14.0) and DVC-6 M (78 ± 16.1) groups compared with the control and SF groups ($p<0.05$).

Evaluation of collagen matrix preservation (Fig. 2a–g) revealed that only the DCV-6 M group (64.6 ± 4.9%) exhibited values statistically comparable to the non-cryopreserved control (66.1 ± 3.6%; $p>0.05$), indicating effective maintenance of extracellular matrix integrity following warming. In contrast, the SF (75.3 ± 3.3%) and DCV-3 M (69.3 ± 3.0%) groups showed significantly higher collagen proportions ($p<0.05$), suggesting potential alterations in

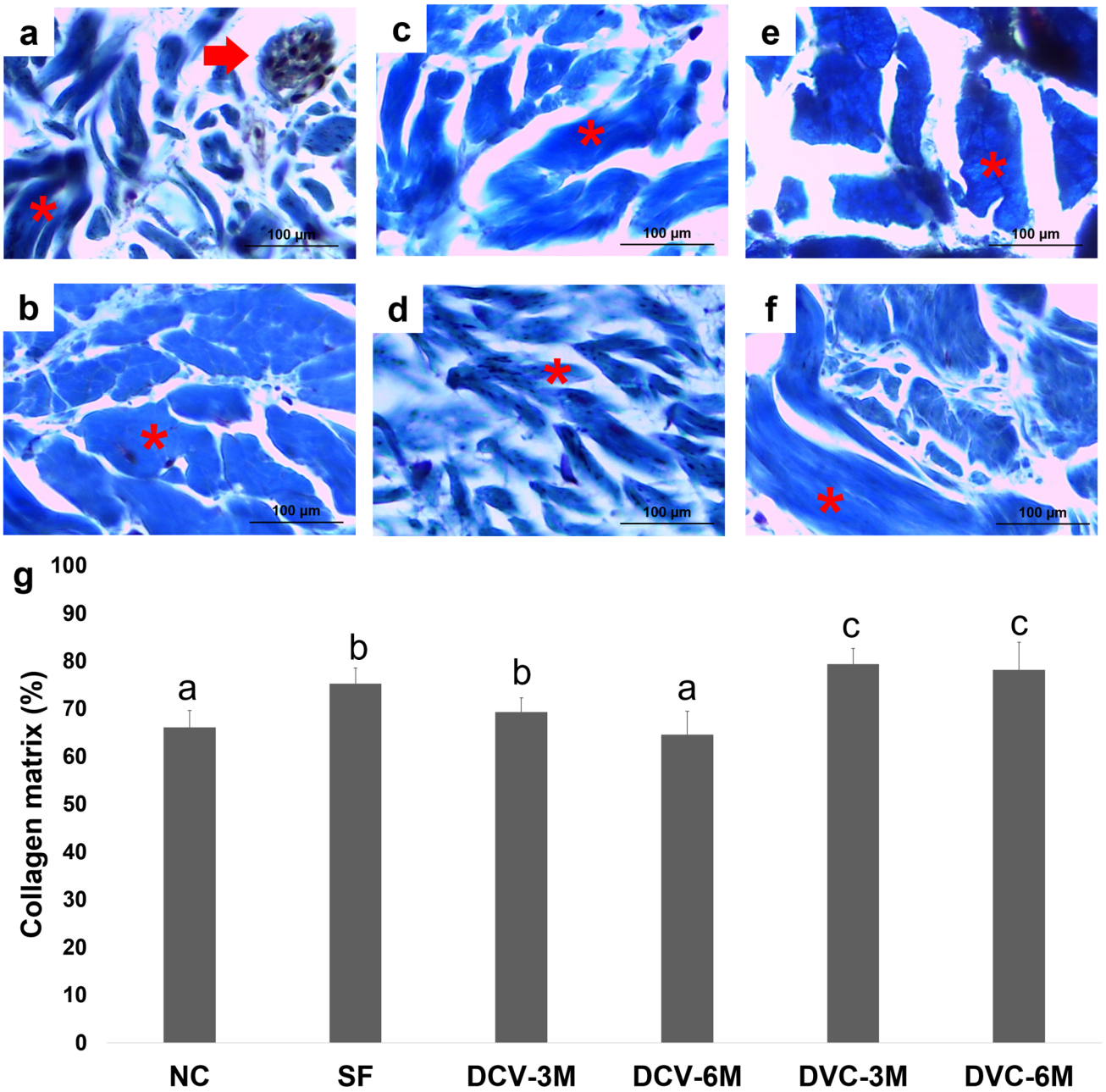


Fig. 2 Representative Masson's trichrome-stained sections of the dermis of Antillean manatees showing the collagen matrix following different tissue preservation methods: **a** non-cryopreserved (NC), **b** slow freezing (SF), **c** direct cover vitrification using 3 M cryoprotectant (DCV-3 M), **d** direct cover vitrification using 6 M cryoprotectant (DCV-6 M), **e** direct vitrification in cryovials using 3 M cryoprotectant (DVC-3 M), and **f** direct vitrification in cryovials using 6 M cryoprotectant (DVC-6 M). **g** Quantification of the collagen matrix in the dermis of NC and cryopreserved groups. Red arrow indicate nerve, and red asterisks indicate the collagen matrix. Different superscript letters indicate statistically significant differences among groups ($p < 0.05$). Scale bar = 100 µm, Magnification 40×

collagen organization or compaction induced by these preservation methods. More pronounced changes were observed in tissues preserved by DVC. Both DVC-3 M (79.4 ± 3.3%) and DVC-6 M (78.2 ± 5.8%) groups exhibited markedly increased collagen content compared with all other experimental groups ($p < 0.05$).

Regarding elastic fibers evaluation (Fig. 3a–g), all vitrification protocols maintained normal elastic fiber organization (DCV-3 M: 0.2 ± 0.0%; DCV-6 M: 0.3 ± 0.1%; DVC-3 M: 0.1 ± 0.1%; DVC-6 M: 0.3 ± 0.1%) similar to non-cryopreserved tissues (0.2 ± 0.2%) and tissues cryopreserved by SF (0.2 ± 0.0%, $p > 0.05$).

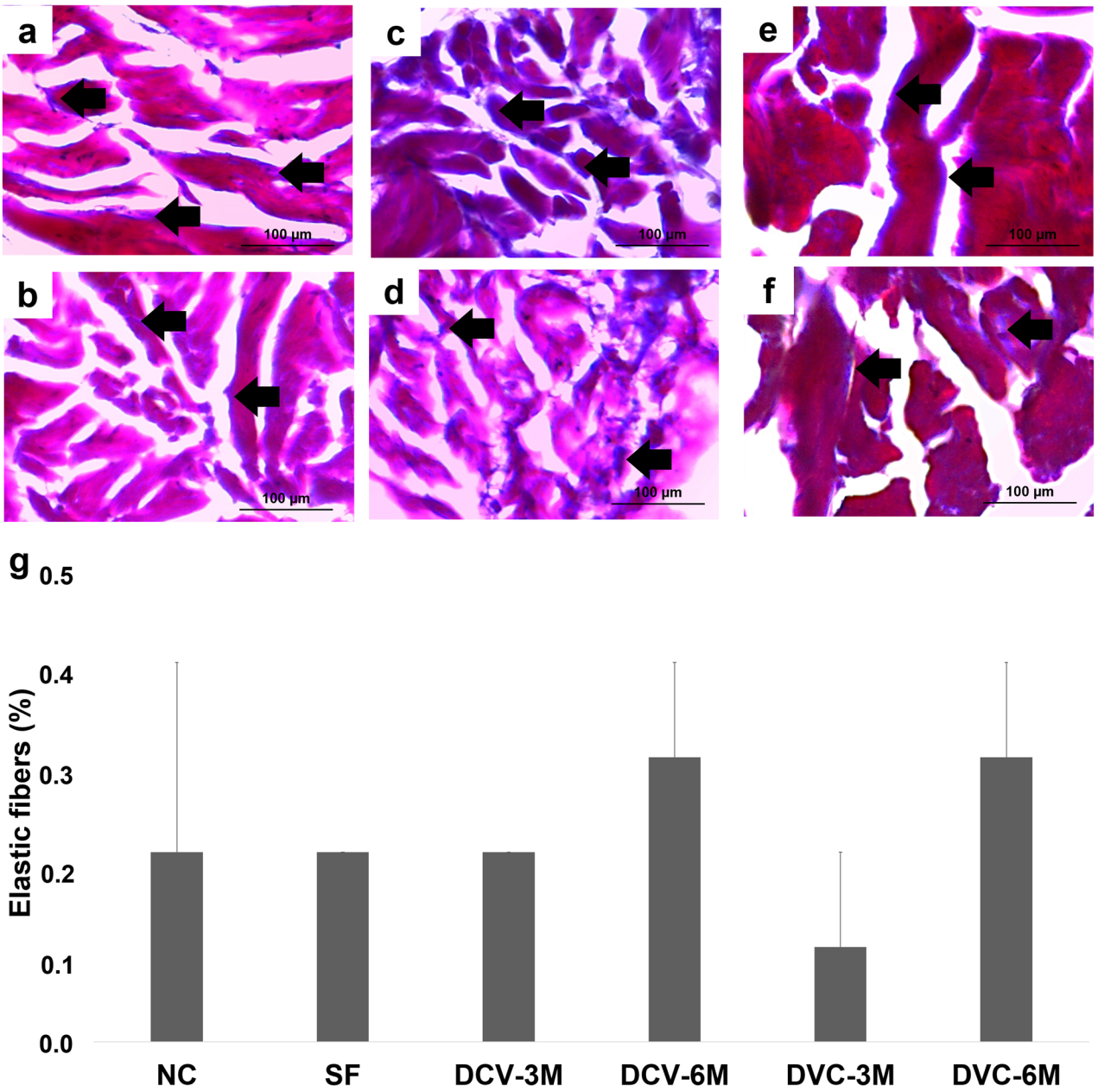


Fig. 3 Representative Weigert's trichrome-stained sections of the dermis of Antillean manatees showing elastic fibers following different tissue preservation methods: **a** non-cryopreserved (NC), **b** slow freezing (SF), **c** direct cover vitrification using 3 M cryoprotectant (DCV-3 M), **d** direct cover vitrification using 6 M cryoprotectant (DCV-6 M), **e** direct vitrification in cryovials using 3 M cryoprotectant (DVC-3 M), and **f** direct vitrification in cryovials using 6 M cryoprotectant (DVC-6 M). **g** Quantification of elastic fiber abundance in the dermis of NC and cryopreserved groups. Black arrows indicate elastic fibers. No statistically significant differences were detected among groups ($p > 0.05$). Scale bar = 100 µm, Magnification 40×

Effects of vitrification techniques on ultrastructural aspects

Scanning electron micrographs (Fig. 4a–f) of dermal tissue from all experimental groups revealed a dense extracellular matrix predominantly composed of well-organized collagen fibers arranged in compact bundles. The fibers exhibited a largely parallel orientation, resulting in a continuous, homogeneous fibrillar pattern with no apparent fragmentation or disorganization. This uniform ultrastructural arrangement indicates satisfactory preservation of dermal architecture and overall tissue morphological integrity across the evaluated groups.

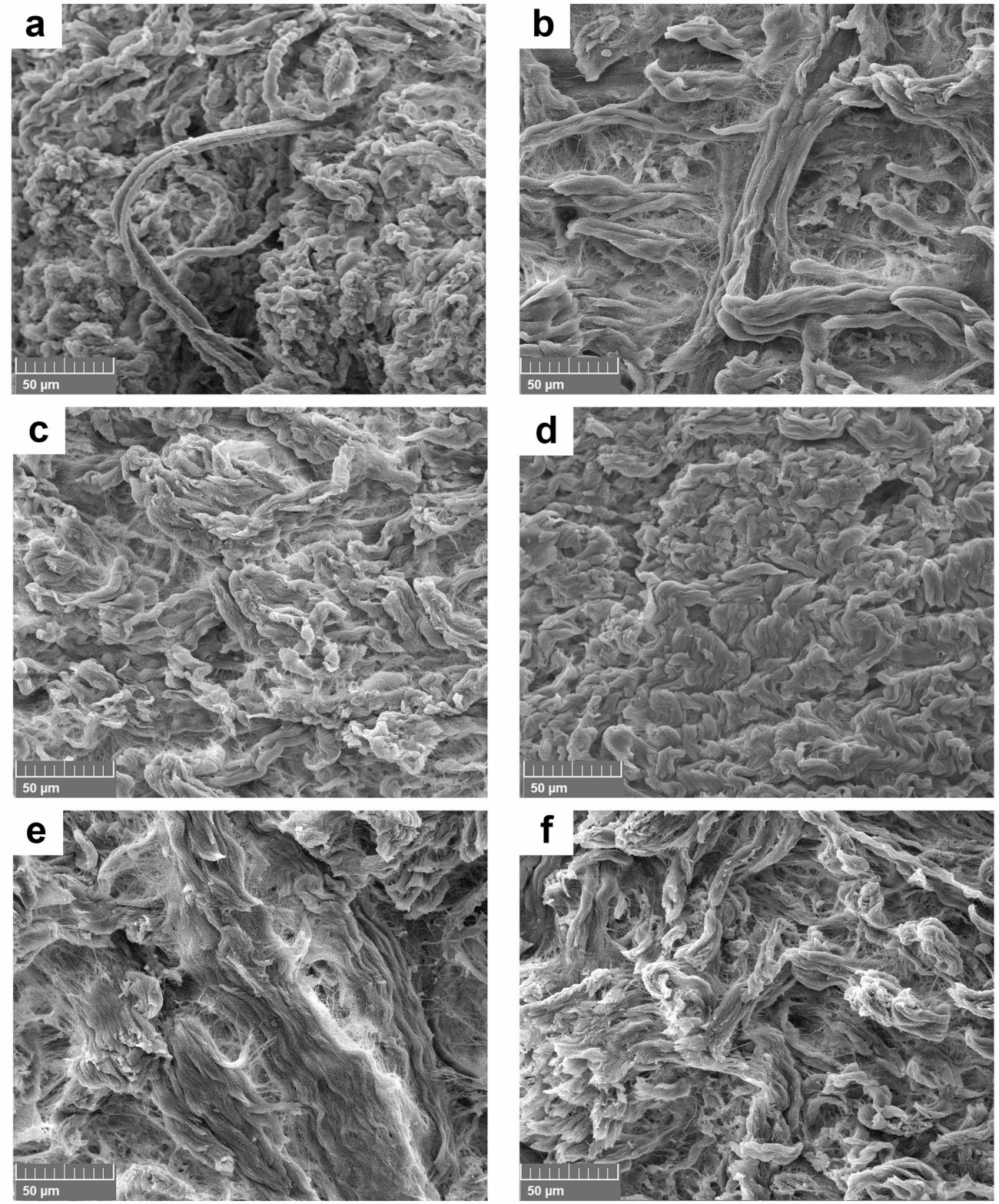


Fig. 4 Representative scanning electron micrographs of Antillean manatee dermal tissue following different preservation methods: **a** non-cryopreserved (NC), **b** slow freezing (SF), **c** direct cover vitrification using 3 M cryoprotectant (DCV-3 M), **d** direct cover vitrification using 6 M cryoprotectant (DCV-6 M), **e** direct vitrification in cryovials using 3 M cryoprotectant (DVC-3 M), and **f** direct vitrification in cryovials using 6 M cryoprotectant (DVC-6 M). The micrographs illustrate the ultrastructural features of the dermal tissue after each preservation treatment. Scale bar = 50 µm

Effects of vitrification techniques on culture and fibroblast aspects

According to the primary in vitro culture evaluation, both non-cryopreserved and SF groups were able to release viable cells that subsequently migrated from the tissue fragments (Fig. 5a–f). However, the samples subjected to both DCV-3 M and DCV-6 M (Fig. 6a–d) and both DVC-3 M and DVC-6 M (Fig. 6e–h) could not detach cells in culture. As shown in Fig. 5, the cells exhibited a spindle shape with long cytoplasmic projections, resembling fibroblasts. All explants in all groups were attached within one day of culture ($p > 0.05$). Still, the day with cell growth around all fragments was observed at 8.4 and 9.3 days in the non-cryopreserved and SF groups, respectively, and was similar between the groups ($p > 0.05$). Additionally, total subconfluent time was 17.9 and 24 in the non-cryopreserved and SF groups, respectively ($p > 0.05$; Table 1).

Discussion

The accelerated loss of biodiversity, particularly among marine species, has intensified discussions about implementing cryobanking strategies. When integrated with assisted reproductive technologies, cryobanks represent a powerful tool to mitigate genetic erosion by preserving germplasm and enabling the future reintroduction of genetic diversity into small, fragmented, or isolated populations (Brereton et al. 2025; Nascimento et al. 2023b). For the Antillean manatee, previous studies have demonstrated that slow freezing is an effective approach for preserving somatic tissues, supporting post-thaw cell viability and recovery (Nascimento et al. 2023b). In contrast, and in agreement with the present findings, vitrification protocols evaluated to date have consistently failed to promote successful fibroblast recovery in culture, highlighting the challenges associated with applying vitrification to manatee dermal tissues.

These findings are noteworthy, as vitrification has been widely reported to produce superior outcomes in the cryopreservation of somatic tissues from several terrestrial

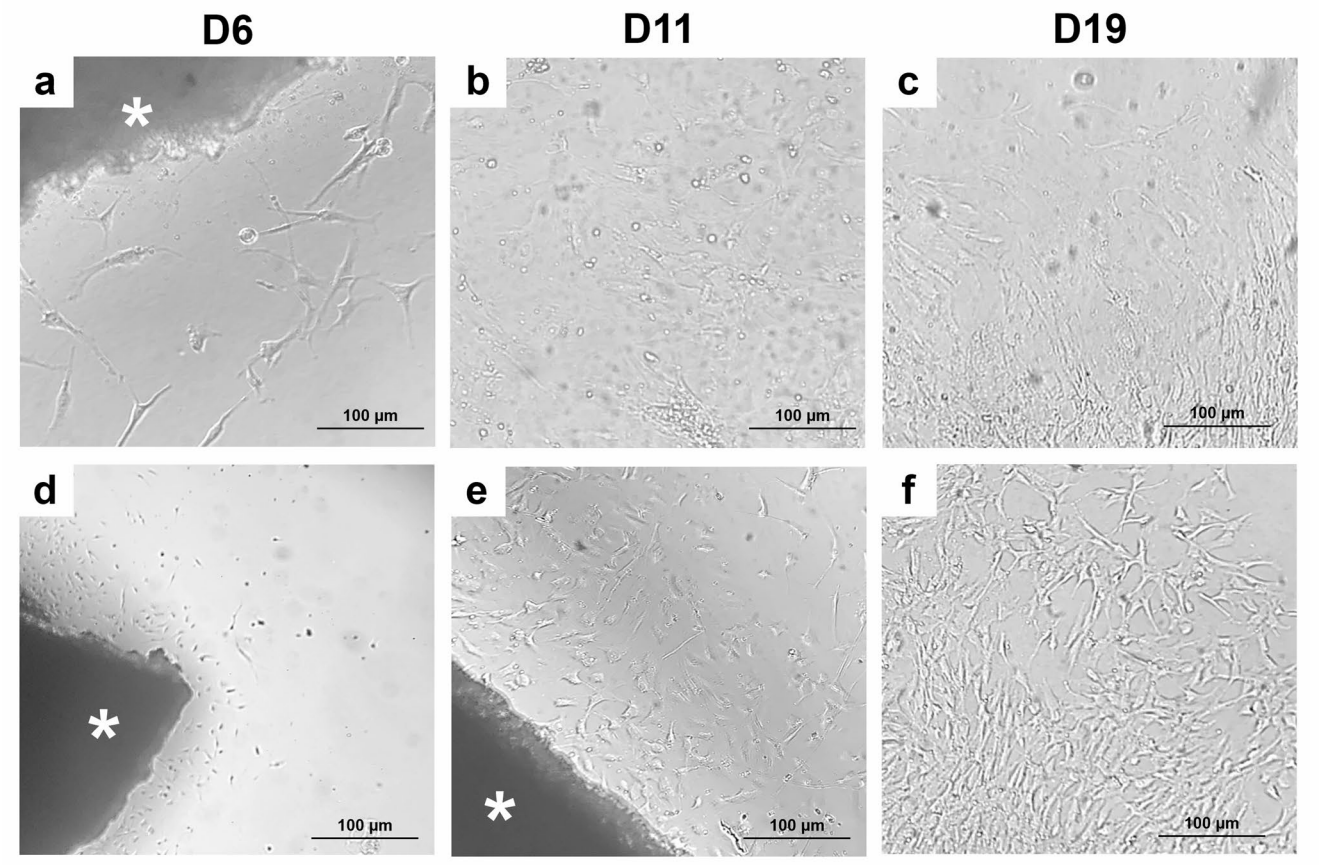


Fig. 5 Representative images showing the in vitro culture of tissue explants from non-cryopreserved (NC) and slow-frozen (SF) Antillean manatee dermal samples following thawing. **a**–**c** NC samples showing tissue attachment and progressive cellular outgrowth at day 6 (D6), day 11 (D11), and day 19 (D19), respectively. **d**–**f** SF samples showing tissue attachment and progressive cellular outgrowth at D6, D11, and D19, respectively. Asterisks indicate tissue explants attached to the culture dishes. Scale bar = 100 µm

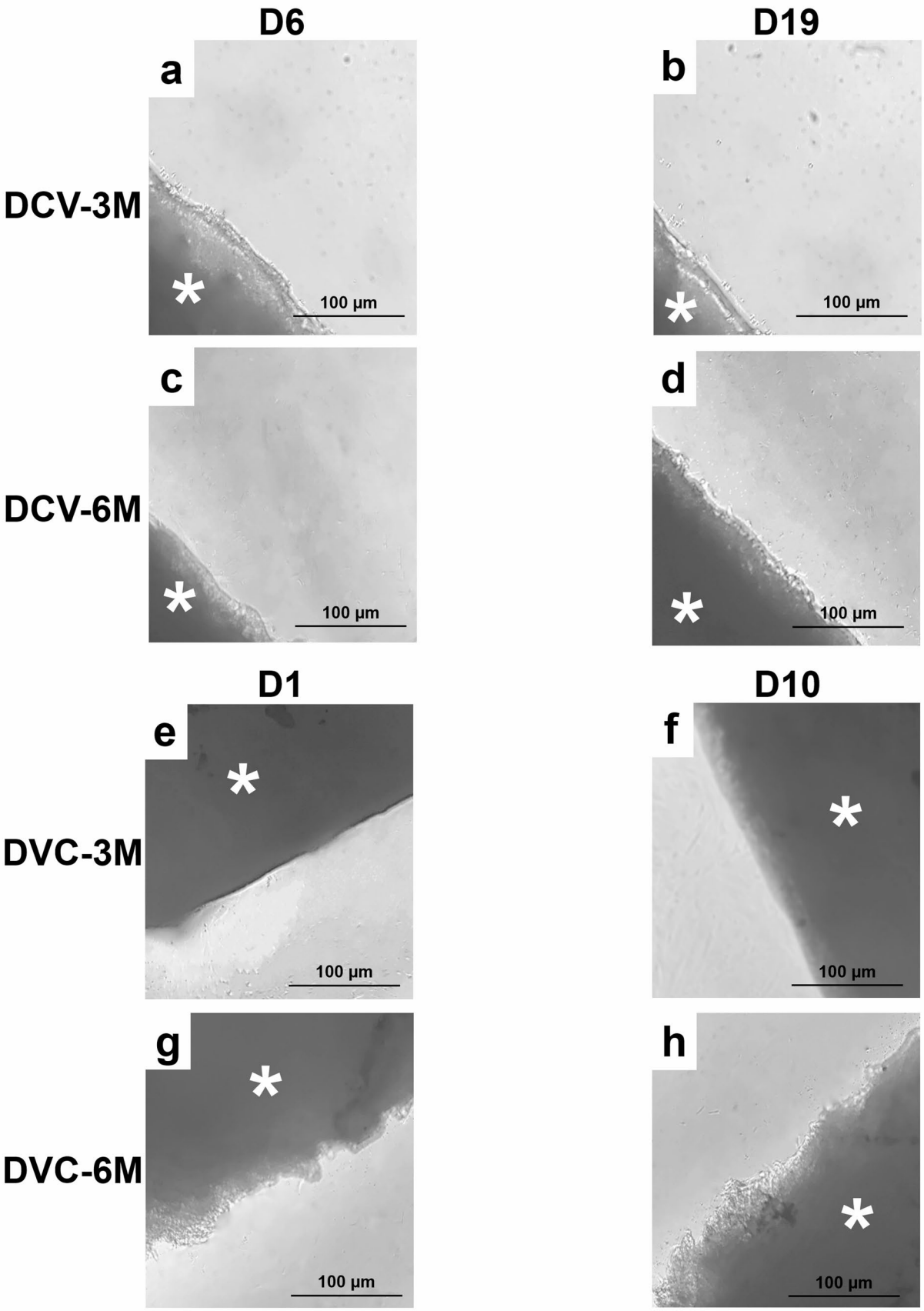

D6
D19
a
b
DCV-3M
*
100 μm
*
100 μm
c
d
DCV-6M
*
100 μm
*
100 μm
D1
D10
e
f
DVC-3M
*
100 μm
*
100 μm
g
h
DVC-6M
*
100 μm
*
100 μm

Fig. 6 Representative images showing the in vitro culture of vitrified Antillean manatee dermal explants following warming, with no evidence of tissue detachment during the culture period. **a**, **b** Direct cover vitrification using 3 M cryoprotectant (DCV-3 M) at day 6 (D6) and day 19 (D19), respectively; **c**, **d** direct cover vitrification using 6 M cryoprotectant (DCV-6 M) at day 1 (D1) and day 10 (D10), respectively; **e**, **f** direct vitrification in cryovials using 3 M cryoprotectant (DVC-3 M) at D1 and D10, respectively; and **g**, **h** direct vitrification in cryovials using 6 M cryoprotectant (DVC-6 M) at D1 and D10, respectively. Asterisks indicate tissue explants attached to the culture dishes. Scale bar = 100 µm

mammals, including the collared peccary (*Pecari tajacu*) (Borges et al. 2017), jaguar (*Panthera onca*) (Praxedes et al. 2019), red-rumped agouti (*Dasyprocta leporina*) (Costa et al. 2020), and puma (*Puma concolor*) (Lira et al. 2021). However, it is important to emphasize that these studies were conducted in terrestrial species, whereas aquatic mammals exhibit distinct anatomical and physiological adaptations that may influence cryopreservation outcomes. Sirenians, including manatees and dugongs, are characterized by thick, hairless skin supported by an extensive blubber layer, which plays a central role in buoyancy and thermoregulation (Bertolesi et al. 2025). As tropical mammals with relatively low metabolic rates and limited tolerance to cold, manatees are particularly susceptible to cold stress syndrome when exposed to water temperatures below 20 °C for extended periods (Hardy et al. 2019; Western et al. 2024). These unique evolutionary and physiological traits may increase the sensitivity of manatee dermal tissue to rapid or subtle thermal fluctuations during vitrification. Consequently, vitrification protocols that are effective in terrestrial mammals may not be directly transferable to sirenians, potentially explaining the reduced efficiency observed in the present study.

For successful future applications, a thorough understanding of dermal histology, in vitro culture processes, and the factors influencing tissue properties is essential (Moura et al. 2024). In this context, histological and ultrastructural analyses provide valuable insights into tissue integrity, as they reveal morphological characteristics closely associated with biological function and adaptive processes (Lima et al. 2026). This is particularly relevant for the Antillean manatee, whose tissues exhibit specialized morphological features related to species-specific adaptations (Melo et al. 2024). Regarding H&E staining, the fibroblast quantification shows preservation of fibroblast density in the DCV groups, with values comparable to those of non-cryopreserved and SF-cryopreserved tissues, suggesting that these protocols are effective in maintaining the quantity of this cell type. This outcome indicates that both SF and DCV may mitigate the deleterious effects typically associated with ice crystal formation and osmotic imbalance during cooling and warming. In contrast, the significant reduction in fibroblast numbers detected in the DVC groups highlights potential limitations of this approach, suggesting that DVC may impose additional physical or chemical stressors that compromise cellular integrity. Also, this decrease suggests that the DVC approach may compromise cellular preservation and negatively affect dermal tissue maintenance regardless of cryoprotectant concentration. Moreover, fibroblast counts in all experimental groups exceeded those reported in previous cryopreservation studies with manatee tissues (Moura et al. 2024; Nascimento et al. 2023a). This discrepancy may be attributed to the younger age of the animals used in the present study, as fibroblast numbers decline with advancing age (Akase et al. 2012).

Similarly, the analysis of collagen matrix preservation revealed clear protocol-dependent effects on extracellular matrix stability. The similarity between DCV-6 M and non-cryopreserved tissues suggests that this condition can maintain collagen integrity after warming, thereby supporting the structural preservation of dermal architecture. Conversely, the significantly higher collagen values detected in the SF and DCV-3 M groups may reflect alterations in matrix organization, potentially associated with collagen fiber compaction or extracellular remodeling induced by cryopreservation stress. The most pronounced alterations were observed in the DVC groups, where both concentrations led to markedly elevated collagen content, suggesting that this technique may exacerbate matrix alterations and compromise tissue homeostasis. These findings indicate that the DVC protocol, irrespective of cryoprotectant concentration, exerts a substantial impact on extracellular matrix preservation, potentially reflecting structural remodeling or densification associated with this vitrification approach. Interestingly, Nascimento et al. (2023a) also observed an increased rate of collagen matrix on cryopreserved tissue of Antillean manatee by SSV when compared to the non-cryopreserved group. These findings highlight the sensitivity of the collagen network to cryopreservation conditions and emphasize the need to refine vitrification protocols to avoid undesirable structural alterations that could limit subsequent applications of preserved tissue.

We also quantified the proportion of elastic fibers to obtain a more complete evaluation of the extracellular matrix. The evaluation of elastic fibers further reinforces the influence of cryopreservation protocols on dermal matrix components. The preservation of baseline values in the SF, DCV, and DVC groups, without significant differences compared to the non-cryopreserved control, suggests that both cryopreservation approaches and the cryoprotective solutions used are effective in maintaining the delicate architecture of elastic fibers, which are particularly susceptible to structural damage during freezing and warming. These results

Table 1 In vitro culture of non-cryopreserved (NC) manatee dermis samples and samples subjected to slow freezing (SF), direct cover vitrification (DCV-3 M and 6 M), and direct vitrification in cryovials (DVC-3 M and 6 M)

Groups	Initial explants	Adhered samples	Adhered samples (%)	Day all fragments adhered	Subconfluent samples	Subconfluent samples (%)	Day with cell growth around all fragments	Total subconfluent time
NC	8.0±0.0	8.0±0.0	1.0±0.0[a]	1.0±0.0[a]	8.0 ± 0.0	1.0±0.0[a]	8.4±0.6[a]	17.9±0.1[a]
SF	4.0±0.0	4.0±0.0	1.0±0.0[a]	1.0±0.0[a]	4.0 ± 0.0	1.0±0.0[a]	9.3±1.8[a]	24.0±0.0[a]
DCV-3M	3.9±0.2	3.6±0.2	0.9±0.1[a]	1.0±0.0[a]	0.0 ± 0.0	0.0±0.0[b]	0.0±0.0[b]	0.0±0.0[b]
DCV-6M	3.7±0.2	3.4±0.2	0.9±0.1[a]	1.0±0.0[a]	0.0 ± 0.0	0.0±0.0[b]	0.0±0.0[b]	0.0±0.0[b]
DVC-3M	3.9±0.1	3.9±0.1	1.0±0.0[a]	1.0±0.0[a]	0.0 ± 0.0	0.0±0.0[b]	0.0±0.0[b]	0.0±0.0[b]
DVC-6M	3.9±0.1	3.9±0.1	1.0±0.0[a]	1.0±0.0[a]	0.0 ± 0.0	0.0±0.0[b]	0.0±0.0[b]	0.0±0.0[b]

[a, b] $p < 0.05$

demonstrated the effective preservation of baseline values under these conditions.

We observed from the histological results that DCV-6 M appears to be more beneficial for tissue structural maintenance; however, we also evaluated the ability of cryopreserved samples to yield somatic cells in vitro. The in vitro culture outcomes demonstrated that only the non-cryopreserved and SF groups generated fibroblast outgrowth, whereas vitrified samples failed to detach cells. The ability of SF-preserved tissues to support cell detachment and proliferation, with culture dynamics comparable to those of fresh controls, underscores their effectiveness in maintaining functional cellular viability. In contrast, the lack of outgrowth in vitrified groups suggests that vitrification conditions may compromise critical cellular processes required for adhesion and proliferation, limiting their applicability for functional tissue recovery.

Recent advances in tissue and organ cryopreservation have highlighted the potential of complex vitrification formulations, such as VS55, VS70, VS83, and M22, for preserving large and structurally complex biological tissues. These formulations have been investigated in the cryopreservation of porcine osteochondral tissues and mammalian kidneys, demonstrating their potential for applications beyond conventional cell cryopreservation (Chen et al. 2023; Han et al. 2023). Importantly, recent evidence indicates that the vitrification properties of cryoprotective solutions may change when they are incorporated into tissues, underscoring the need for tissue-specific optimization of cryoprotectant concentration and loading, as well as cooling and warming rates (Han et al. 2024). Therefore, future studies could investigate whether such vitrification formulations, together with optimized cryoprotectant loading and warming strategies, could improve the preservation of manatee tissues, while carefully considering the increased cytotoxicity associated with the higher cryoprotectant concentrations required for vitrification.

In general, the cytotoxicity of intracellular cryoprotectants represents one of the major challenges to be addressed for the successful establishment of cryopreservation protocols (Raju et al. 2021). Considering the previously reported lack of effectiveness of vitrification for obtaining viable cells (Nascimento et al. 2023a), we tested two cryoprotectant solutions at different concentrations (3 M and 6 M), and the higher concentration appeared to be more suitable. The primary distinction between SF and vitrification lies in the concentration of cryoprotectants and the cooling rate, with vitrification typically requiring higher concentrations to be effective (Jaiswal and Vagga 2022). In addition to cryoprotectant concentration, factors such as cooling and warming rates, sample volume, and viscosity are critical determinants of vitrification efficiency and should be considered before choosing a protocol (Pegg 2002). Among these factors, the age and sex of different animals can alter their morphological and physiological patterns, suggesting that these factors may affect the technique's efficiency (Emmerson and Hardman 2012; Felician et al. 2018).

The results of this study demonstrate that the efficiency of cryopreservation techniques for Antillean manatee skin-derived samples is highly dependent on the method and cryoprotectant combination used. Histological assessments revealed that SF and DCV protocols preserved fibroblast density and maintained tissue architecture at levels comparable to non-cryopreserved controls. In contrast, DVC resulted in significant cell loss, suggesting deleterious effects on cellular integrity. Similarly, extracellular matrix analyses indicated that while DCV, particularly at 6 M, promoted stable preservation of collagen and elastic fibers, DVC was associated with marked alterations in collagen content. These findings highlight that, despite overall preservation of dermal ultrastructure observed under scanning electron microscopy, subtle yet biologically relevant changes in cellular and matrix parameters were protocol-dependent. Furthermore, the inability of vitrified samples to produce viable fibroblasts in vitro, in contrast to the successful outgrowth observed in non-cryopreserved and SF groups, emphasizes the challenges in translating vitrification outcomes into functional tissue recovery.

Conclusions

Among the vitrification methods tested, DCV, particularly at higher cryoprotectant concentrations, maintained tissue architecture and preserved matrix components, whereas DVC was associated with significant reductions in fibroblast density and marked alterations in collagen matrix. Moreover, none of the vitrification protocols supported fibroblast proliferation in vitro, underscoring the challenges of applying this approach to manatee tissues. Slow freezing proved effective in preserving fibroblast viability and extracellular matrix integrity, and in supporting in vitro cell outgrowth, with outcomes comparable to those of the non-cryopreserved control. Together, these results highlight slow freezing as the most reliable technique currently available for this species, while also indicating the need to refine vitrification strategies further to minimize cytotoxic effects and structural alterations. Such advances are essential for developing optimized cryobanking protocols that support long-term conservation efforts for the Antillean manatee and can be carried out under field conditions.

Acknowledgements The authors thank the CMA/ICMBio for making the animals used in this research available. This study was financed by the Coordenação de Aperfeiçoamento de Pessoal de Nível Superior – Brazil (CAPES, Financial Code 001) and Conselho Nacional de Desenvolvimento Científico e Tecnológico (CNPq, 304536/2026-1 and 403312/2025-6). MF Oliveira and AF Pereira are recipients of CNPq grants.

Author contributions L.L.V. Rodrigues: Conceptualization, Methodology, Validation, Investigation, Data curation, Writing—Original draft & Review. L.V.C. Aquino: Methodology, Investigation. P.R.R. Assunção: Methodology, Investigation. Y.L.F. Silva: Methodology, Investigation. V.D. Silva: Methodology, Investigation. M.V.O. Santos: Methodology, Investigation. R.E.M. Oliveira: Methodology, Investigation. M.F. Oliveira: Methodology, Investigation. F.O. Luan: Methodology, Investigation. F.L.N. Attademo: Methodology, Investigation. A.F. Pereira: Conceptualization, Methodology, Validation, Formal analysis, Resources, Writing—Original draft & Review, Writing—Review & Editing, Supervision, Funding acquisition.

Funding The Article Processing Charge (APC) for the publication of this research was funded by the Coordenação de Aperfeiçoamento de Pessoal de Nível Superior - Brasil (CAPES) (ROR identifier: 00x0ma614).

Data availability No datasets were generated or analysed during the current study.

Declarations

Conflict of interest The authors declare that they have no conflict of interest.

Open Access This article is licensed under a Creative Commons Attribution 4.0 International License, which permits use, sharing, adaptation, distribution and reproduction in any medium or format, as long as you give appropriate credit to the original author(s) and the source, provide a link to the Creative Commons licence, and indicate if changes were made. The images or other third party material in this article are included in the article's Creative Commons licence, unless indicated otherwise in a credit line to the material. If material is not included in the article's Creative Commons licence and your intended use is not permitted by statutory regulation or exceeds the permitted use, you will need to obtain permission directly from the copyright holder. To view a copy of this licence, visit http://creativecommons.org/licenses/by/4.0/.

References

Akase T, Nagase T, Huang L, Ibuki A, Minematsu T, Nakagami G, Ohta Y, Shimada T, Aburada M, Sugama J, Sanada H (2012) Aging-like skin changes induced by ultraviolet irradiation in an animal model of metabolic syndrome. Biol Res Nurs 14(2):180–187. https://doi.org/10.1177/1099800411401013

Amini M, Benson JD (2023) Technologies for vitrification based cryopreservation. Bioengineering 10(5):508. https://doi.org/10.3390/bioengineering10050508

Anikienko IV, Ryadinskaya NI, Petrov EA, Kostyunin KY, Belova SE, Ikonnikova DR (2025) Skin of the Baikal seal (*Pusa sibirica*, Phocidae): norm and pathology. Biol Bull 52(11):316. https://doi.org/10.1134/S1062359025700621

Aquino LVC, Olindo SL, Silva YLF, Oliveira LRM, Moura YBF, Rodrigues ALR, Praxedes ÉA, Oliveira MF, Silva AR, Pereira AF (2024) Cryopreservation and passaging optimization for *Galea spixii* (Wagler, 1831) adult skin fibroblast lines: A step forward in species management and genetic studies. Acta Histochem 126(5–7):152185. https://doi.org/10.1016/j.acthis.2024.152185

Bertolesi GE, Heshami N, McFarlane S (2025) Evolutionary adaptations of TRPA1 thermosensitivity and skin thermoregulation in vertebrates. Iscience 28(9):113369. https://doi.org/10.1016/j.isci.2025.113369

Borges AA, Lima GL, Queiroz-Neta LB, Santos MVO, Oliveira MF, Silva AR, Pereira AF (2017) Conservation of somatic tissue derived from collared peccaries (*Pecari tajacu* Linnaeus, 1758) using direct or solid-surface vitrification techniques. Cytotechnology 69(4):643–654. https://doi.org/10.1007/s10616-017-0074-7

Boroda AV, Kipryushina YO, Golochvastova RV, Shevchenko OG, Shulgina MA, Efimova KV, Katin IO, Maiorova MA (2020) Isolation, characterization, and ecotoxicological application of marine mammal skin fibroblast cultures. Vitro Cell Dev Biol – Anim 56(9):744–759. https://doi.org/10.1007/s11626-020-00506-w

Brereton JE, Spooner SL, Walker SL, Mooney A, Wilson P, Mastromonaco GF, Hunter E, White S (2025) When to cryopreserve and when to let it go? A systematic review of priorities in wild animal cryobanking. Theriogenol Wild 6:100119. https://doi.org/10.1016/j.therwi.2025.100119

Chen P, Wang S, Chen Z, Ren P, Hepfer RG, Greene ED, Campbell LH, Helke KL, Nie X, Jensen JH, Hill C, Wu Y, Brockbank KGM, Yao H (2023) Nanowarming and ice-free cryopreservation of large sized, intact porcine articular cartilage. Commun Biol 6:220. https://doi.org/10.1038/s42003-023-04577-9

Costa CA, Borges AA, Nascimento MB, Aquino LVC, Silva AR, Oliveira MF, Pereira AF (2020) Effects of vitrification techniques on the somatic tissue preservation of agouti (*Dasyprocta leporina* Linnaeus, 1758). Biopreserv Biobank 18(3):165–170. https://doi.org/10.1089/bio.2019.0109

Emmerson E, Hardman MJ (2012) The role of estrogen deficiency in skin ageing and wound healing. Biogerontology 13(1):3–20. https://doi.org/10.1007/s10522-011-9322-y

Engdawork A, Belayhun T, Aseged T (2024) The role of reproductive technologies and cryopreservation of genetic materials in the conservation of animal genetic resources. Ecol Genet Genom 31:100250. https://doi.org/10.1016/j.egg.2024.100250

Felician FF, Xia C, Qi W, Xu H (2018) Collagen from marine biological sources and medical applications. Chem Biodivers 15(5):e1700557. https://doi.org/10.1002/cbdv.201700557

Fernandes DP, Praxedes ÉA, Viana JVS, Aquino LVC, Rodrigues LLV, Moura YBF, Oliveira MF, Freitas CIA, Pereira AF (2023) Influence of cryopreservation techniques and low concentrations of permeating cryoprotectants on the conservation of ear cartilage and skin derived from six-banded armadillos (*Euphractus sexcinctus* Linnaeus, 1758). Cryobiology 113:104788. https://doi.org/10.1016/j.cryobiol.2023.104788

Gao Y, Jin S, Wang J (2026) Protein and peptide-based strategies for advanced cryopreservation. ChemBioChem 27(2):e202500889. https://doi.org/10.1002/cbic.202500889

Han Z, Rao JS, Gangwar L, Namsrai BE, Pasek-Allen JL, Etheridge ML, Wolf SM, Pruett TL, Bischof JC, Finger EB (2023) Vitrification and nanowarming enable long-term organ cryopreservation and life-sustaining kidney transplantation in a rat model. Nat Commun 14:3407. https://doi.org/10.1038/s41467-023-38824-8

Han Z, Gangwar L, Namsrai BE, Rao JS, Scheithauer C, Etheridge ML, Finger EB, Bischof JC, Choi J (2024) Kidney tissue loading reduces the critical cooling and warming rates of VS55 and VMP cryoprotective solutions. Cryobiology 117:104977. https://doi.org/10.1016/j.cryobiol.2024.104977

Hardy SK, Deutsch CJ, Cross TA, Wit M, Hostetler JA (2019) Cold-related Florida manatee mortality in relation to air and water temperatures. PLoS ONE 14(11):e0225048. https://doi.org/10.1371/journal.pone.0225048

Jaiswal AN, Vagga A (2022) Cryopreservation: a review article. Cureus 14:31564. https://doi.org/10.7759/cureus.31564

Lima MA, Oliveira REM, Attademo FLN, Oliveira RM, Pereira AIA, Silva FJL, Farias DSD, Gavilan AS, Pereira AF, Huser-Davis RA, Oliveira MF (2026) Lingual surface morphology in delphinids: structural adaptations to feeding strategies. Microsc Microanal 32(3):ozag045. https://doi.org/10.1093/mam/ozag045

Lira GPO, Borges AA, Nascimento MB, Aquino LVC, Moura LFMP, Silva HVR, Ribeiro LR, Oliveira MF, Pereira AF (2021) Effects of somatic tissue cryopreservation on puma (*Puma concolor* L, 1771) tissue integrity and cell preservation after *in vitro* culture. Cryobiology 101:52–60. https://doi.org/10.1016/j.cryobiol.2021.06.003

Melo LIS, Oliveira REM, Sousa ACFC, Oliveira RM, Lima MA, Fragoso ABL, Silva FFL, Attademo FLN, Luna FO, Pereira AF, Oliveira MF (2024) Antillean manatee (*Trichechus manatus manatus* Linnaeus, 1758) tongue morphology and adaptive herbivorous implications. Microsc Microanal 30:160–168. https://doi.org/10.1093/micmic/ozad135

Morales-Vela B, Quintana-Rizzo E, Mignucci-Giannoni A (2024) Trichechus manatus ssp. manatus. IUCN Red List Threat Species 2024:eT22105A43793924. https://doi.org/10.2305/IUCN.UK.2024-2.RLTS.T22105A43793924.en

Moura YBF, Aquino LVC, Nascimento MB, Oliveira REM, Attademo FLN, Luna FO, Pereira AF (2024) Age and sex effects on histological features and *in vitro* culturing of Antillean manatee (*Trichechus manatus manatus*, Linnaeus 1758) dermis. Anat Histol Embryol 53(4):e13081. https://doi.org/10.1111/ahe.13081

Nascimento MB, Moura YBF, Oliveira REM, Borges AA, Oliveira MF, Luna FO, Attademo FLN, Pereira AF (2023a) Influence of intracellular cryoprotectants on the conservation of dermal somatic tissues derived from Antillean manatees (*Trichechus manatus manatus* Linnaeus, 1758). Biopreserv Biobank 21(5):483–492. https://doi.org/10.1089/bio.2022.0044

Nascimento MB, Moura YBF, Oliveira REM, Lira GPO, Borges AA, Luna FO, Attademo FLN, Pereira AF (2023b) The initial steps toward the formation of somatic tissue banks and cell cultures derived from captive Antillean manatee (*Trichechus manatus manatus*) skin biopsies. Zoo Biol 42(6):709–722. https://doi.org/10.1002/zoo.21798

Olindo SL, Aquino LVC, Moura YBF, Silva YLF, Rodrigues ALR, Silva VD, Pereira AF (2024) Investigating cryopreservation techniques for maintaining morphology and *in vitro* viability of cartilage and skin from Spix's yellow-toothed cavies (*Galea spixii* Wagler, 1831) for conservation through biobanks. J Mol Histol 55(6):1199–1209. https://doi.org/10.1007/s10735-024-10259-5

Pan S, Zhang A (2026) Effect of cooling rate on the quality of biological samples during cryopreservation. Int J Refrig 183:419–430. https://doi.org/10.1016/j.ijrefrig.2026.01.020

Pegg DE (2002) The history and principles of cryopreservation. Semin Reprod Med 20(01):005–014.

Praxedes ÉA, Oliveira LRM, Silva MB, Borges AA, Santos MVO, Silva HVR, Oliveira MF, Silva AR, Pereira AF (2019) Effects of cryopreservation techniques on the preservation of ear skin–An alternative approach to conservation of jaguar, *Panthera onca* (Linnaeus, 1758). Cryobiology 88:15–22. https://doi.org/10.1016/j.cryobiol.2019.04.007

Raju R, Bryant SJ, Wilkinson BL, Bryant G (2021) The need for novel cryoprotectants and cryopreservation protocols: Insights into the importance of biophysical investigation and cell permeability. Biochim Biophys Acta - Gen Subj 1865(1):129749. https://doi.org/10.1016/j.bbagen.2020.129749

Rodrigues LLV, Oliveira LRM, Moura YBF, Silva YLF, Viana JVS, Aquino LVC, Oliveira REM, Attademo FLN, Luna FO, Pereira AF (2025b) Efficient cryopreservation of Antillean manatee skin-derived somatic cells via reduced intracellular cryoprotectant concentration. Vitro Cell Dev Biol - Anim 62:378–388. https://doi.org/10.1007/s11626-025-01061-y

Rodrigues LLV, Oliveira REM, Attademo FLN, Pereira AF (2025a) The role of skin-derived somatic cell and tissue cryobanks in the conservation of aquatic mammals. Biopreserv Biobank 23(2):79–88. https://doi.org/10.1089/bio.2023.0168

Su CY, Liu TY, Wang HV, Yang WC (2023) Histopathological study on collagen in full-thickness wound healing in Fraser's dolphins (*Lagenodelphis hosei*). Animals 13(10):1681. https://doi.org/10.3390/ani13101681

Val HG, Attademo FL, Normande IC, Borges JCG, Costa AF, Alencar AEB, Melo LIS, Paiva-Jr LH, Luna FO (2024) Influence of sex and home range on released Antillean manatees' behavior in Brazil. Lat Am J Aquat Mamm 19(1):7–14. https://doi.org/10.5597/lajam00325

Viana JVS, Moura LFMP, Praxedes ÉA, Aquino LVC, Nascimento MB, Prazeres-Júnior FR, Oliveira MF, Pereira AF (2023) Effects of vitrification techniques on the formation of skin cryobank of the ocelot (*Leopardus pardalis*). CryoLetters 44(1):47–56. https://doi.org/10.54680/fr23110110412

Western JL, Hieb EE, Russell ML, Clark CD, Rotstein DS, Perry SM, Ingrisano A, Carmichael RH, Stacy NI, Bloodgood JC (2024) Cold stress, heart failure, and esophageal occlusion cause the death of a West Indian manatee *Trichechus manatus* in Alabama, USA. Dis Aquat Org 160:57–63. https://doi.org/10.3354/dao03824

Zhang X, Liu X, Liu XL, Wu DY, Zhou K, Yu ZS, Dou C, Xu T, Yu M, Miao YL (2023) Preserving porcine genetics: a simple and effective method for on-site cryopreservation of ear tissue using direct cover vitrification. Int J Mol Sci 24(8):7469. https://doi.org/10.3390/ijms24087469

Publisher's note Springer Nature remains neutral with regard to jurisdictional claims in published maps and institutional affiliations.